Regional hydrologic and ecologic characterization and baseline assessment of remote northern Canadian terrain in advance of shale oil and gas development

Seventh Annual Report to:

NWT ESRF Management Board

By:

David Rudolph

University of Waterloo

April, 2024

1.0 Introduction

During the 2023-2024 field and research period, project activities remained on a no-cost extension to the initial 5-year ESRF project. During the 2023 field season, the research team was able to re-visit the Bogg Creek watershed field site. Access was not possible during the 2 previous years but during spring 2022, the airborne electromagnetic geophysical survey (AEM) was flown over the field site, with initial results being presented in the 2022 Annual Report. The focus during the past year included 4 main areas, three of which were new initiatives and two were continuing from previous years. The first of the new activities involved the collection of shallow soil cores at several locations to further characterize subsurface soil conditions and permafrost water content and mineralogy. In concert with the soil coring, soil gas emissions were collected with surface flux chambers and soil gas probes with the specific intent to analyze the carbon composition and age of soil gas leaving the ground surface at several locations within the study area. The second new activity was related to the application of terrestrial Electrical Resistivity Tomography (ERT), Ground Conductivity Meter (GCM), and Ground Penetrating Radar (GPR) at a series of targeted locations within the watershed area. Ongoing work included advancing the interpretation of the AEM survey data with new software and ground truth data and continuing development and application of numerical modeling tools for simulating freeze-thaw processes within the discontinuous permafrost landscape. The modeling work continues to explore the influence of transient groundwater flow phenomena on surface water systems, land form change and ecology and has been extended to accommodate solute fate and reactive transport during permafrost thaw.

The work remains focused within the Bogg Creek watershed, near Norman Wells in the Central Mackenzie Valley (CMV), NWT. Three graduate students, Ms. Jiaqi Weng (PhD, U. Waterloo) (modeling), Mr. Oliver Conway-White (PhD, U. Waterloo) (geophysics) and Mr. Hugo Crites (PhD, U of Ottawa) (carbon fate and transport) have been working on the main components of the project and their work over the course of the past year forms a considerable part of the Year 7 annual report. Cenovus Energy continues to support the research activities and Mr. Chris Salewich remained as our main collaborator from Cenovus during Year 7. Mr. Salewich has recently left Cenovus and new contacts are being established for subsequent collaborative work. Progress on the project and a proposal for a Phase 2 of the research program was presented to the ESRB virtually on November 21, 2023 and a project update was presented to Cenovus personnel on March 15, 2024.

The project continues to receive additional technical, financial and in-kind support from research colleagues at Wilfrid Laurier University (WLU) and Cenovus. Leveraged financial and in-kind support continues to be provided through our on-going participation in the Global Water Futures (GWF) program and specifically the Northern Water Futures project headed by Dr. Jenn Baltzer at WLU. This report provides a summary of the research results obtained during Year 7 along with a summary of relevant presentations and publications.

2.0 Airborne Geophysical Survey

The airborne electromagnetic geophysical survey (AEM) survey completed in May 2022 remains a source of continued evaluation and interpretation. In depth analysis of the survey results using various data modeling and processing approaches continues to provide new insight. The work presented here, completed during the Year 7 period is largely the work of PhD student Mr. Oliver Conway-White.

2.1 Hydrogeologic control on permafrost revealed by airborne frequency-domain electromagnetics

The interaction of permafrost with geology and hydrology in the Bogg Creek watershed was evaluated using an airborne frequency-domain electromagnetic (FDEM) survey together with borehole-derived ice observations (Figure 1). The airborne FDEM survey was completed using the Resolve6™ system and consisted of 1091 line kilometers with 70 m spacing. The survey was completed as two blocks, one in the southeast which covers the road and a section of the Mackenzie River, and one in the northwest which incorporates a diverse assortment of lakes and streams. The survey was flown over three days in May 2022. Inverted resistivity models were assessed to map permafrost distribution, both laterally and vertically, within this discontinuous permafrost region in both unconsolidated sediments and bedrock (Figure 2). Resistivity results were interpreted using permafrost depths and considered in relation to landscape features from regional satellite images and geological maps. A summary of these interpretations is provided below.

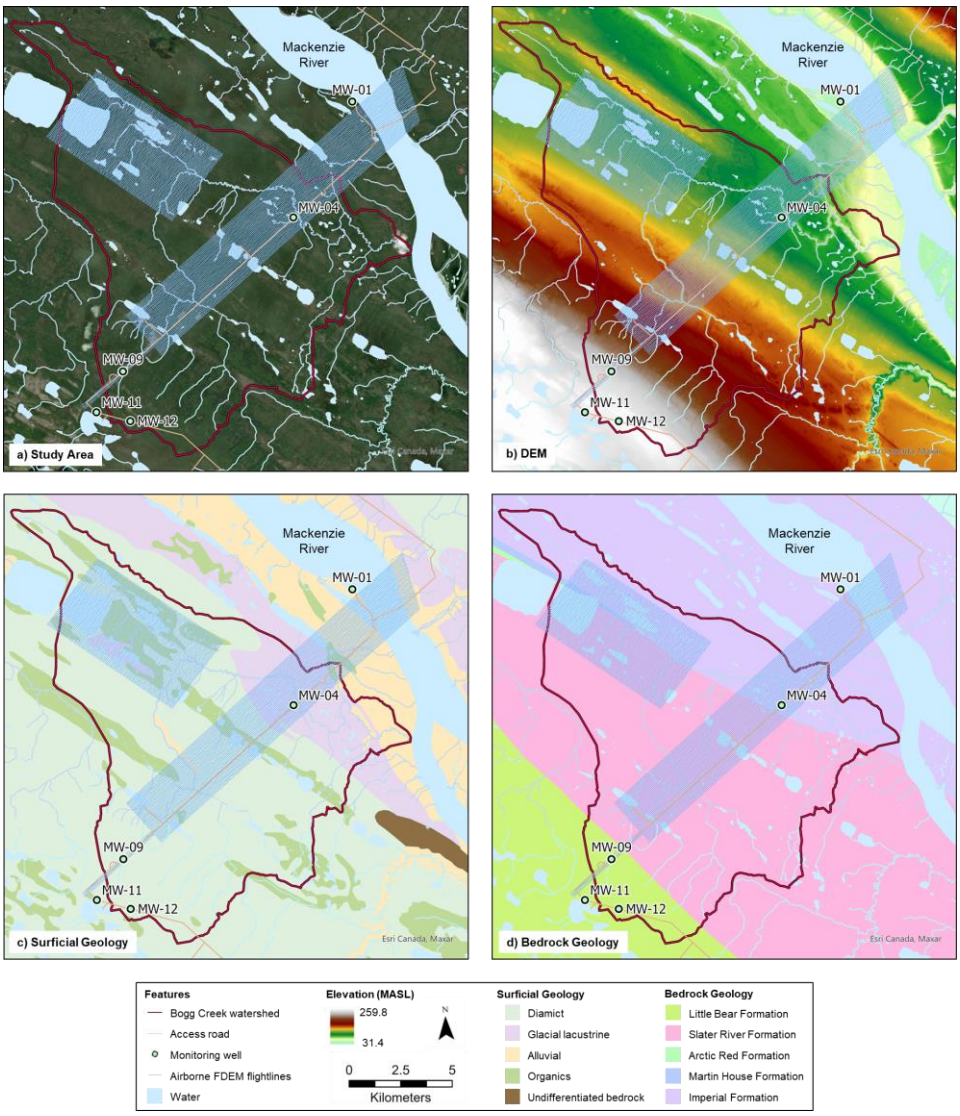

Figure 1. a) Topographic map of study area showing key site features including extent of Bogg Creek Watershed, surface waterbodies, monitoring well locations, access road, and FDEM survey lines. b) Digital

Elevation Model of study site shows elevation decreasing from the southwest to the Mackenzie River in the northwest (Porter et al., 2023). c) Surficial geology of the study area is dominated by clay- and silt-rich diamicts and sand and gravel colluvial and alluvial sediments (modified from Côté et al., 2013). d) Bedrock geology of the study area consists of predominately shales (Imperial and Slater River formations) and sandstones (Little Bear Formation) (modified from Fallas et al., 2013; Fallas and McNaughton, 2013).

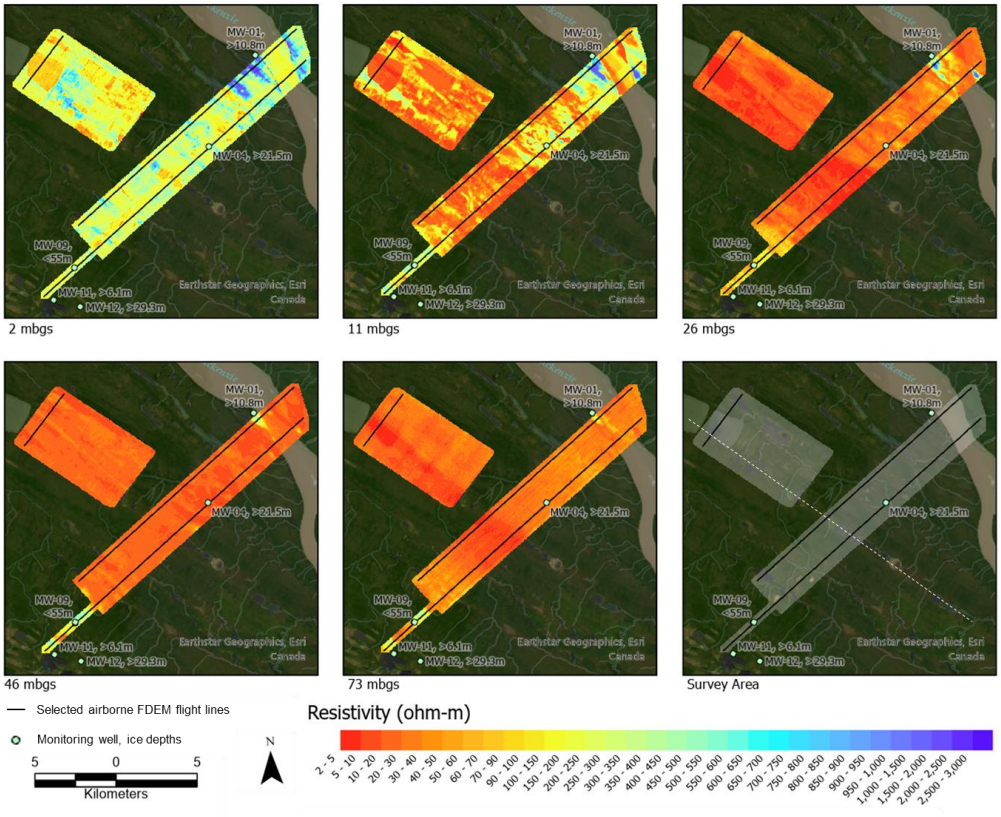

Figure 2. Selected depth slices through inverted resistivity model. The uppermost slice reveals the highest resistivities, with the most resistive unit (blue) becomes increasingly discontinuous with depth. High resistivity persists downward in both the northeast around the Mackenzie River and the southwest portion of the study area. White dashed line highlights orthogonal lake system which is hypothesized to be controlled by the underlying structural geology of the area.

2.2 Geologic controls on permafrost distribution

Resistivity results for depths from 2 to 20 m are shown with mapped distribution of coarse grained alluvial, fine grained lacustrine, and poorly sorted diamictons, with organic peat deposits concentrated in lower topographic areas (Figure 3). The lateral variability at 2 mbgs shows the resistivity ranges of frozen unconsolidated sediments (<5 ohm-m to >1000 ohm-m), with most of the area having resistivity values that would be greater than typical sediment ranges expected for unfrozen saturated materials (i.e., >250 ohm-m) (Herring et al., 2023). It has been suggested that permafrost may be most extensive in finer-grained sediments (e.g., Holloway and Lewkowicz, 2020), a trend only partially observed here with permafrost coverage seen to be greatest in both coarse- and fine-grained sediments. Distribution of organic soils and landcover may play a greater role in permafrost distribution than direct sediment texture.

Adjacent to the Mackenzie River, a high resistivity zone (>300 ohm-m) extends towards the bottom of the resistivity model (Figure 4). Given the extremely high resistivity of this anomaly compared to what would be expected for an unfrozen shale (i.e., Imperial Formation), it is anticipated that this represents a region of frozen bedrock. Moving southwest away from the river, this resistive anomaly thins rapidly. The resistivity change is inferred as a decrease in permafrost thickness. The bottom of this resistive anomaly is anticipated to represent the base of the permafrost, which varies from approximately 0 to 20 m. At the southwest edge of the study area, a distinct increase in resistivity is observed within the bedrock, with resistivity values >600 ohm-m which is corroborated with the base of the permafrost observed at MW-09 (Figure 4).

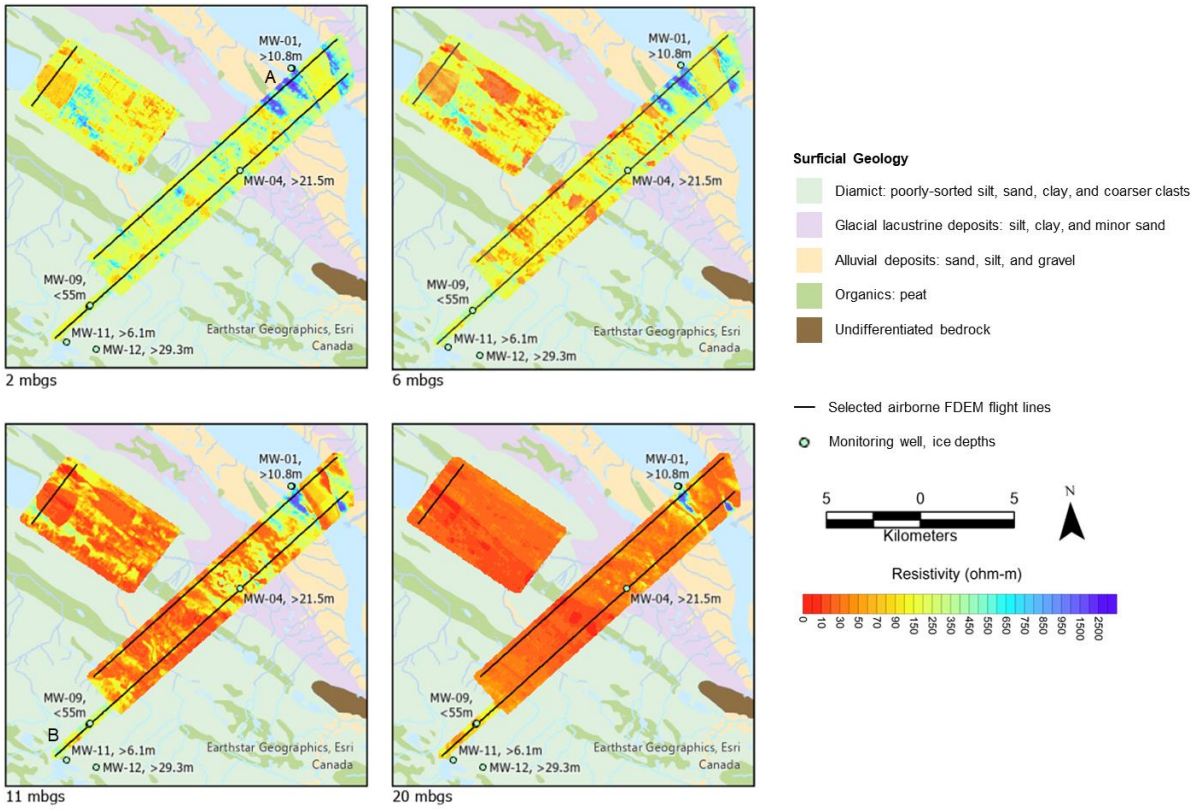

Figure 3. Inverted resistivity depth slices over surficial geology. Permafrost is inferred to occur in all major surficial sediment units and is seen to be relatively variable. However, permafrost is inferred to occur most consistently in the alluvial sediments and the lacustrine sediments based on the higher resistivities observed in these areas. The diamicton unit generally displays a thinner inferred permafrost layer. High resistivity zones discussed in the text are indicated by A and B.

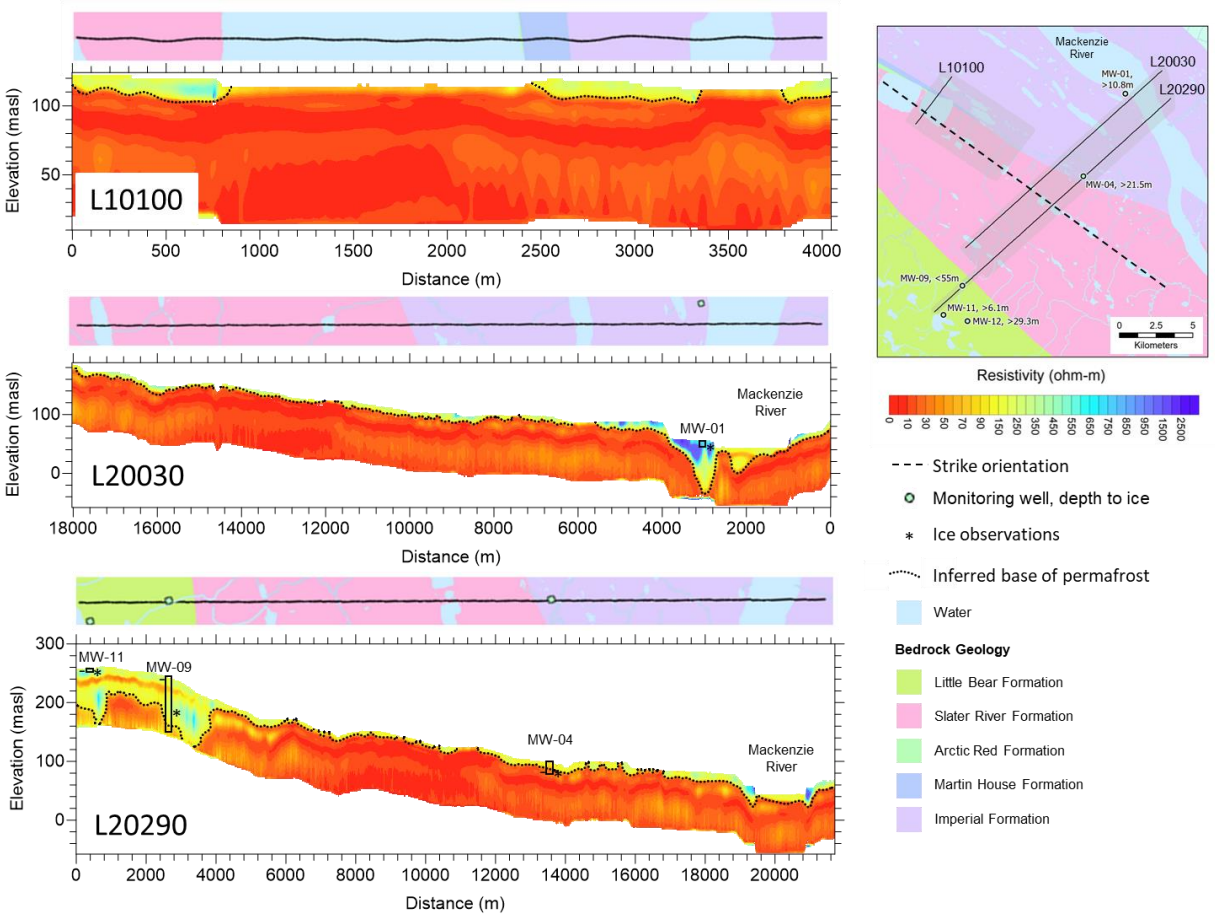

Figure 4. Inferred base of permafrost along selected flight lines. Higher resistivities, inferred as permafrost, occur as a largely continuous layer along most of the transects. Most discontinuities observed in this frozen region occur directly over surface water bodies. Near the Mackenzie River along L20030, and in the southwest of L20290, high resistivity anomalies are observed to extend towards the bottom of the model and are inferred as areas of thicker permafrost. High resistivity zones discussed in the text are indicated by A and B. (bedrock geology modified from Fallas et al., 2013; Fallas and McNaughton, 2013).

2.3 Hydrogeological influence on permafrost distribution

Discontinuities within the permafrost are observed to be predominantly associated with surface water bodies (Figure 2 and 4), with low resistivities extending to surface (red) beneath some of these features associated with thawing of permafrost. Many thawed regions below lakes appear to extend entirely through the unconsolidated sediments and into the bedrock, indicating a through talik. Within the centre of the study area, a chain of orthogonal lakes occurs in a line parallel to the hinge of a syncline that defines the bedrock structure in the area (Figure 4). Given the low permeability of the shale matrix, it is hypothesized that groundwater flow would be primarily through bedrock fractures and joints, vertically connecting deeper groundwater and surface water and forming through taliks in this area. This contrasts with the southwest and northeast portions of the study area where deeply frozen bedrock may impede groundwater connection with surface.

Despite the absence of permafrost beneath larger waterbodies, the resistivity model reveals increased resistivity immediately adjacent to some lakes (e.g., L10100 in Figure 4). These resistive zones may indicate permafrost thickening or increased sediment ice content adjacent to through talik regions. This observation suggests a relatively isolated impact on permafrost thaw from surface water bodies. It is hypothesized that the presence of frozen sediments directly around lakes, as opposed to a uniform thawed region extending directly outwards from the lake, may indicate that vertical groundwater exchange (either recharge or discharge) has a greater influence on permafrost thaw than changes in thermal regime caused by a lack of vegetation or solar warming of the water. This observation of permafrost continuity surrounding waterbodies could, have important implications for the hydrological system in these environments.

The Mackenzie River is surrounded by anomalously high resistivities (e.g., L20030 in Figure 4), indicating extensive ice content both around, and potentially beneath, sections of the river. An important implication of this observation would be that groundwater discharge into the Mackenzie River in these frozen areas could be lower or more isolated than expected from regional hydrogeological conceptualizations of the area.

2.4 Permafrost delineation in complex terrains

Detailed understanding of northern watersheds is challenging in discontinuous permafrost zones due to the limited availability of high-resolution spatial data on permafrost distribution. In these areas, permafrost may vary from non-existent to tens or hundreds of metres thick over relatively small lateral distances making these data crucial for informing modelling studies. The airborne FDEM technique presented allows watershed-wide distribution of permafrost in both unconsolidated sediments and bedrock to be resolved. Of note, the AEM survey method allowed identification of permafrost base depth, a parameter that is otherwise difficult or impossible to assess in discontinuous permafrost regions using conventional methods (e.g., boreholes and surface-based geophysics). Insights of permafrost distribution within bedrock environments are lacking in the literature, making such measurements valuable for assessing the connection between permafrost, bedrock structures, and northern hydrogeology. The efficiency of AEM data acquisition and interpretation opens the possibility of regular monitoring to gain more insight into permafrost changes with time. AEM surveys offer potential for informing hydrological models required to assess changes in northern watersheds in changing climatic conditions.

3.0 Summary of 2023 Surface Geophysical Fieldwork

Surface geophysical surveys using Electrical Resistivity Tomography (ERT), Ground Conductivity Meter (GCM), and Ground Penetrating Radar (GPR), were conducted at three sites along the Husky access road to investigate permafrost presence and characteristics in relation to different landscape features (Figure 5). Surveys were completed between July 20-24, 2024. Key observations include rapid degradation of permafrost in areas cleared of vegetation, and the complex association of permafrost and surface hydrological features in the area. Preliminary results and interpretations for each method are summarized below.

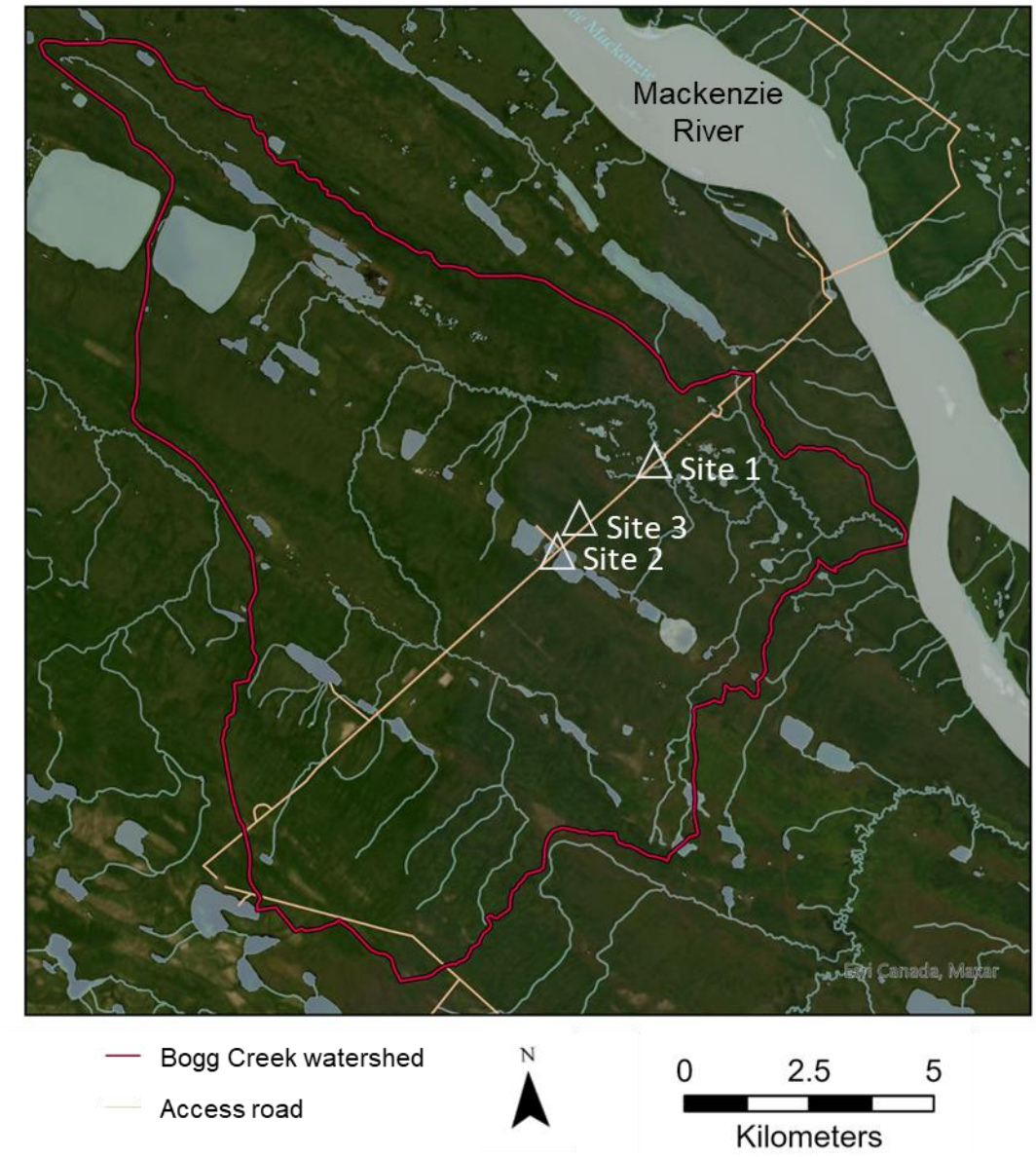

Figure 5. Surface geophysical surveys were completed at three sites (white triangles) within the Bogg Creek watershed. ERT was completed at all three sites while GPR and GCM data was completed at Sites 1 and 3 only.

3.1 Electrical resistivity survey

ERT surveys were complete using a Syscal Pro Switch (Iris Instruments, Orleans, France) with a 96 electrode multicore cable at all three locations. A dipole-dipole array was selected for its strength in resolving vertical changes in subsurface resistivity. The array configuration also allows multiple measurement and reading sets to be completed simultaneously, allowing efficient data acquisition. Surveys were collected using either 1 m or 5 m electrode spacing, yielding depths of investigation of approximately 20 m and 100 m, respectively. Pre-processing of apparent resistivity measurements involved data merging and removal of erroneous potentials. Resistivity inversions were completed using RES2DINV (Geotomo Software, Malaysia), which uses the Gauss–Newton least-squares method and a

robust inversion scheme (L_1-norm). Due to the marked increase in resistivity associated with the transition of unfrozen to frozen sediments, permafrost distribution could be interpreted.

- Site 1 – Drill Pad Clearing

Two perpendicular lines crossing at the centre of the of the drill pad were completed using the high-resolution 1 m electrode spacing (Figure 6a). Inverted resistivity shows a sharp decrease in resistivity going from the forested area into the clearing. This resistivity contrast is interpreted as a transition from frozen to unfrozen soils and is corroborated with data from permafrost probe data collected along the two transects. A highly resistive anomaly was also observed underlying the lower-lying area to the southwest of the road. This area contains a wetland and small stream, suggesting permafrost control on surficial hydrology, with frozen ground potentially impeding infiltration in some areas. Field photos are shown in Figure 8.

- Site 2 – Between Lakes

A 1 km line running along the side of the access road was completed using a 5 m electrode spacing (Figure 6b). The line parallels the road and follows a section of the AEM flightline. The line runs between two lakes which are connected by a wetland area and small stream. Inverted resistivity results show increased resistivity between these lakes, with both an increase in absolute resistivity as well as thickening of the resistive layer compared to the areas further away from the lakes. This may suggest an increase in permafrost extent adjacent to some waterbodies, indicating talik zones surrounding waterbodies have relatively limited lateral extent. As at Site 1, permafrost may control surface water connectivity, potential acting as an impermeable boundary between lakes as well as controlling wetland development. Field photo of survey line is shown in Figure 9.

- Site 3 – Historic Seismic Line Cut

A single 100 m line extending perpendicular to a seismic line was completed using the high-resolution 1 m electrode spacing (Figure 6c). As observed at Site 1, inverted resistivity results show a sharp decrease in resistivity going from the forest into the seismic line where vegetation was previously cleared. Here, the low resistivity zone appears to extend both vertically and laterally, forming a “V” shape below cleared area. The cause of this permafrost degradation pattern will be the study of future study through additional geophysical data collection at seismic lines of different ages and vegetation types, as well as modelling studies.

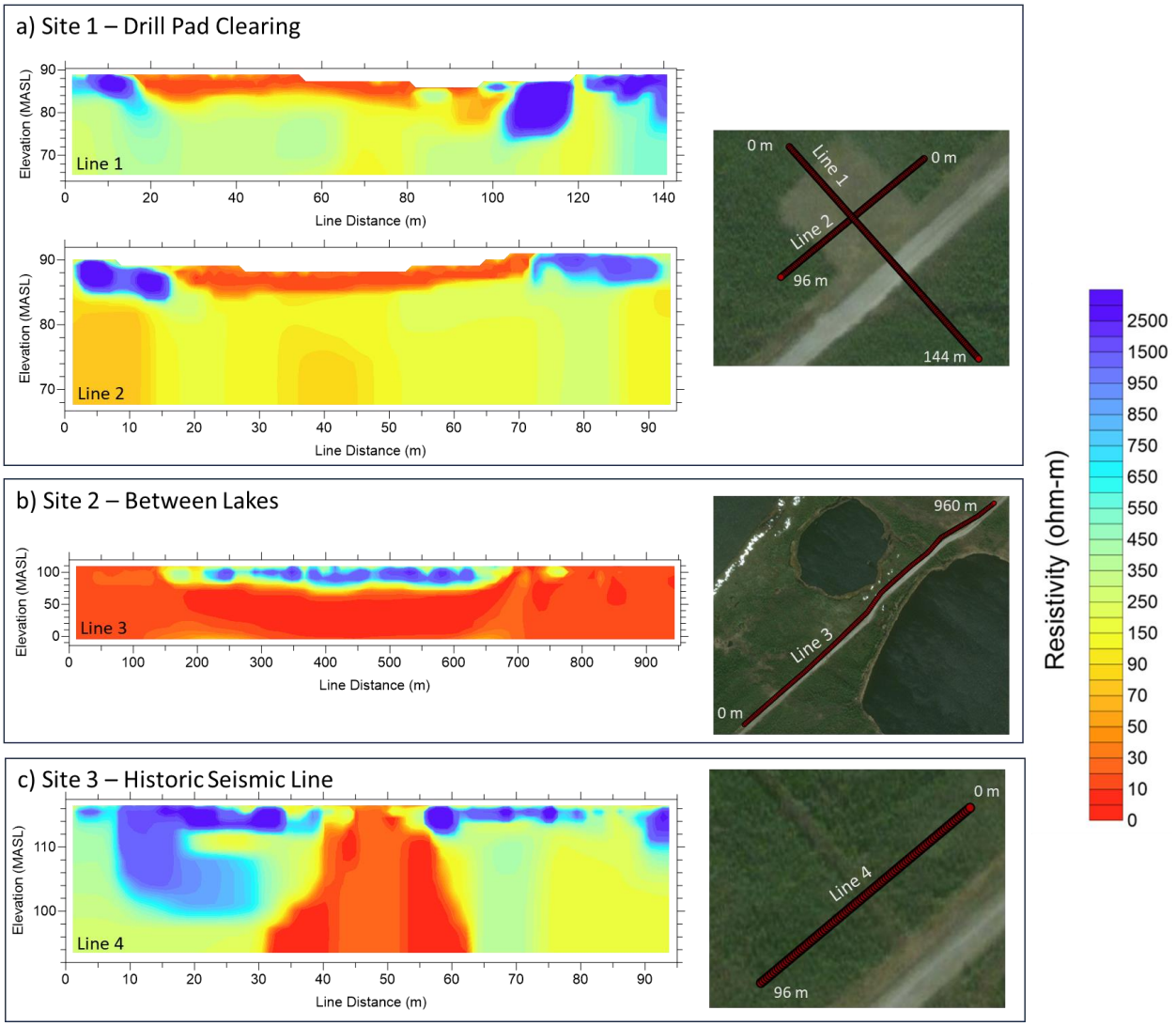

Figure 6. Inverted resistivity models at the three sites. Surveys at sites 1 and 3 were completed with 1 m electrode spacing while the survey at site 2 was completed with 5 m electrode spacings. Warm colours (reds and yellow) represent areas of lower resistivity interpreted as having minimal ground ice content while colour colours (green and blue) are interpreted as areas of permafrost. Permafrost appears to sharply degrade in previously forested areas that were cleared (a and c). Permafrost is interpreted between lakes (b) as well as below wetland areas (southeast of road in a).

3.2 Ground Conductivity Meter – EM 38-4

An EM 38-4 (Geonics, Ontario, Canada) ground conductivity meter was used to investigate the shallow surface at Sites 1 (Drill Pad) and 2 (Seismic Line Cut). The EM 38-4 is an electromagnetic induction method that utilizes 4 coil frequencies, each of which are most sensitive to conductivity changes at different depths. Readings from the different coils are inverted to determine a conductivity model of the upper ~2 m of the subsurface. Here, conductivity was converted to its inverse unit of resistivity for comparison with the ERT transects. Preliminary inversions of the EM 38-4 data were completed using Aarhus Workbench

(Aarhus, Denmark). The EM38-4 requires no contact with the ground and is paired with a backpack GPS unit that allows rapid data collection.

The 2023 field season served as a test of the EM 38-4 instrument, with inverted results demonstrating that the tool can reveal areas of high and low resistivity that correspond to permafrost presence and active zone thickness (Figure 7). These results compare well with the inverted resistivity models from the ERT surveys at the tested locations as well as the permafrost probe data. Given the potential for rapid characterization and the portability of the EM38-4 instrument, this tool is proposed to support future studies targeting seismic line cuts of various ages and other clearings across the region. This tool will allow a larger dataset of locations to be collected than is possible with more detailed methods such as ERT.

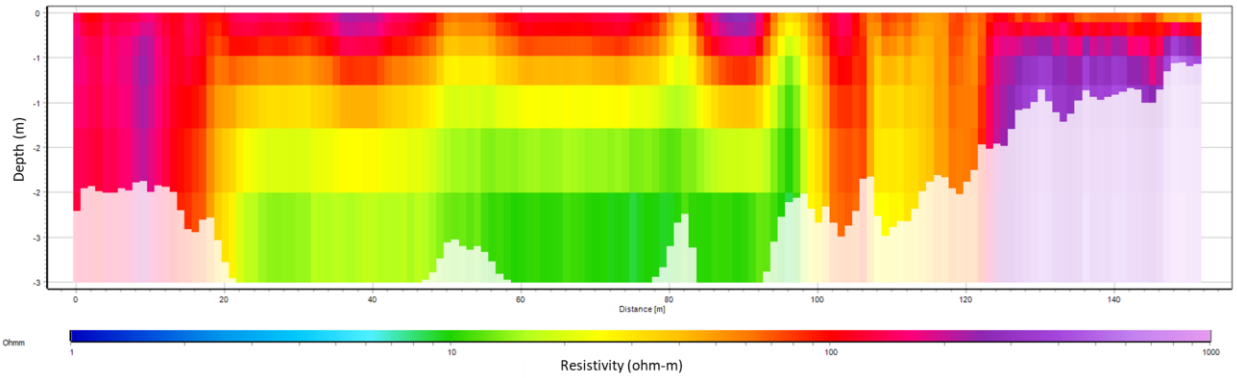

Figure 7. Example inverted model from the EM38-4 GCM for Line 1. Here, lower resistivity (green and yellow) indicate areas of degraded permafrost that were observed within the clearing of the drill pad. The EM38-4 instrument is very portable and allows for rapid acquisition of data.

3.3 Ground Penetrating Radar

GPR data was collected to provide high-resolution characterization of permafrost and soil characteristics and stratigraphy in the upper few metres of the subsurface. The surveys were completed using a pulseEKKO Pro (Sensors and Software System, Ontario, Canada). Shielded 100 MHz antennae were selected to balance resolution with depth of investigation. Reflection profiles were collected along each transect at the well pad and clearing site, as well as several common midpoint soundings (CMPs) which are used to determine the velocity and depth of subsurface materials. Preliminary processing of the GPR data indicates interference from reflections off roots and tree canopy caused significant noise in the datasets, making interpretation difficult. Additional processing and filtering are in progress to improve these results. A field image of the GPR system and survey is shown in Figure 10.

Figure 8. Site 1 showing (left to right) drill pad clearing looking southeast towards the road, forested area to the northwest of the clearing, and wetland area to the southeast of the road.

Figure 9. Site 2. The survey was completed approximately 10 m to the northwest (right-hand side in this photograph) of the road.

Figure 10. GPR equipment in the drill pad clearing at Site 1.

4.0 Overburden Coring and Soil Gas Sampling

In order to provide additional subsurface information to support the interpretation of the terrestrial and air borne geophysical surveys, shallow soil cores were collected at 4 test sites along the all season road (Figure 11). The sediment coring and sol gas work are part of the PhD research of Mr. Hugo Crites from the University of Ottawa. The core samples provided information on the sediment composition in the shallow overburden and permitted the examination of permafrost water content. The core material also provided initial information regarding the amount and composition of carbon within the thawed and frozen sediments, which will help to focus subsequent field investigations regarding the occurrence and type of natural carbon species contained within the shallow subsurface. In addition to the coring activity, soil gas samples were collected at 10 different sites with both a surface gas collection chamber and a conventional soil gas probe. The gas samples will be used to determine the nature of soil gas emissions in this discontinuous permafrost landscape and help to improve estimates of green house gas emissions in a thawing permafrost environment under warming climatic conditions. As part of the field activities, water samples were collected from several local water bodies and where possible, from shallow groundwater for general geochemical analysis and measurement of stable isotopes of oxygen and hydrogen.

The coring and soil gas sampling completed during the 2023 field season were designed to test field sampling techniques and collect initial field data in support of a more focussed field sampling campaign planned for the 2014 field season. A brief explanation of the field methods, sampling locations and some initial results are presented below.

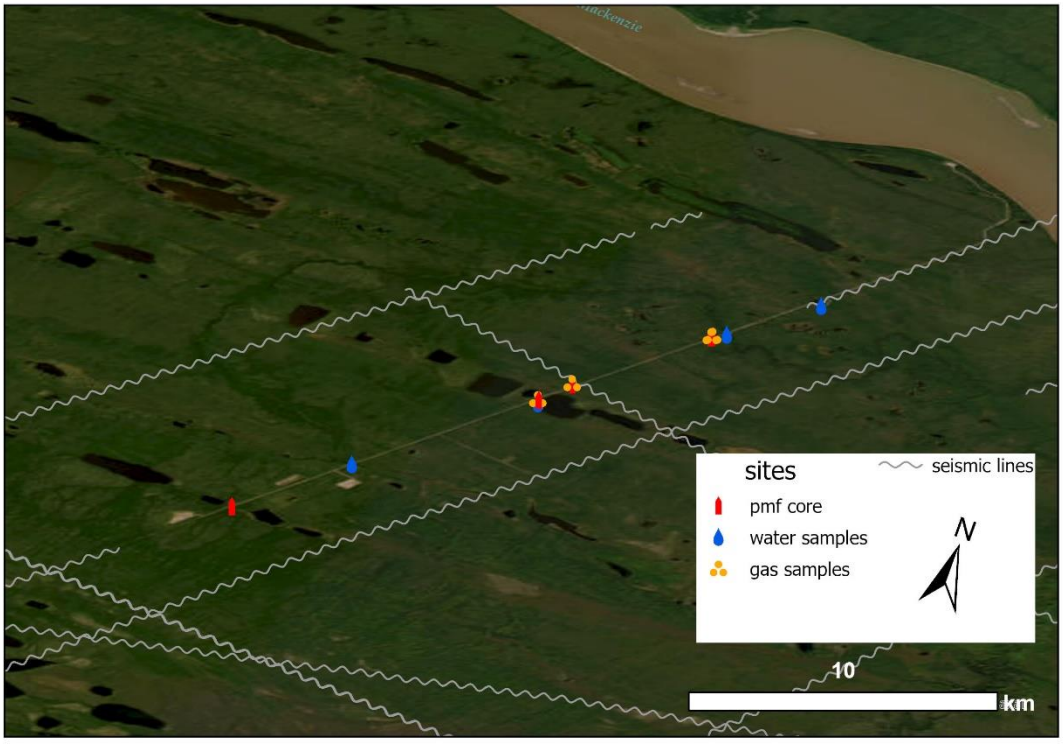

Figure 11. Map of sample collection sites for 2023.

4.1 Soil Coring

The soil core samples were collected using a 1m long, 10 cm diameter portable CRREL permafrost coring system with a gas-powered auger (Figure 12 and Figure 13). The cores were collected through the active zone and into the top of the permafrost, where it was present, to depths ranging from 1 m to 1.5 m. Samples were split into 10 cm subsamples and placed in airtight Ziploc bags and IsoJar™ containers and kept frozen from the time of collection, through shipping to laboratory storage freezers at the University of Ottawa. For this initial testing of the sample collection system, a total of 4 sites were selected: 2 in disturbed landscapes (abandoned well drilling pad and an old seismic line) and 2 control sites in undisturbed, natural vegetation. A conceptual diagram of the coring at the undisturbed and disturbed sites is presented in Figure 14.

The core samples were initially oven-dried at 60°C for 48 hours to determine soil water content. Following the drying step, loss on ignition (LOI) analysis was complete to calculate percentages of inorganic and organic carbon matter present in the permafrost. These data a still being processes. Additional analysis of the core samples to determine the type of carbon within the sediments is now underway.

Figure 12. Permafrost coring setup in undisturbed terrain. Mr. Hugo Crites in the photo with permission.

Figure 13. Example of permafrost core section.

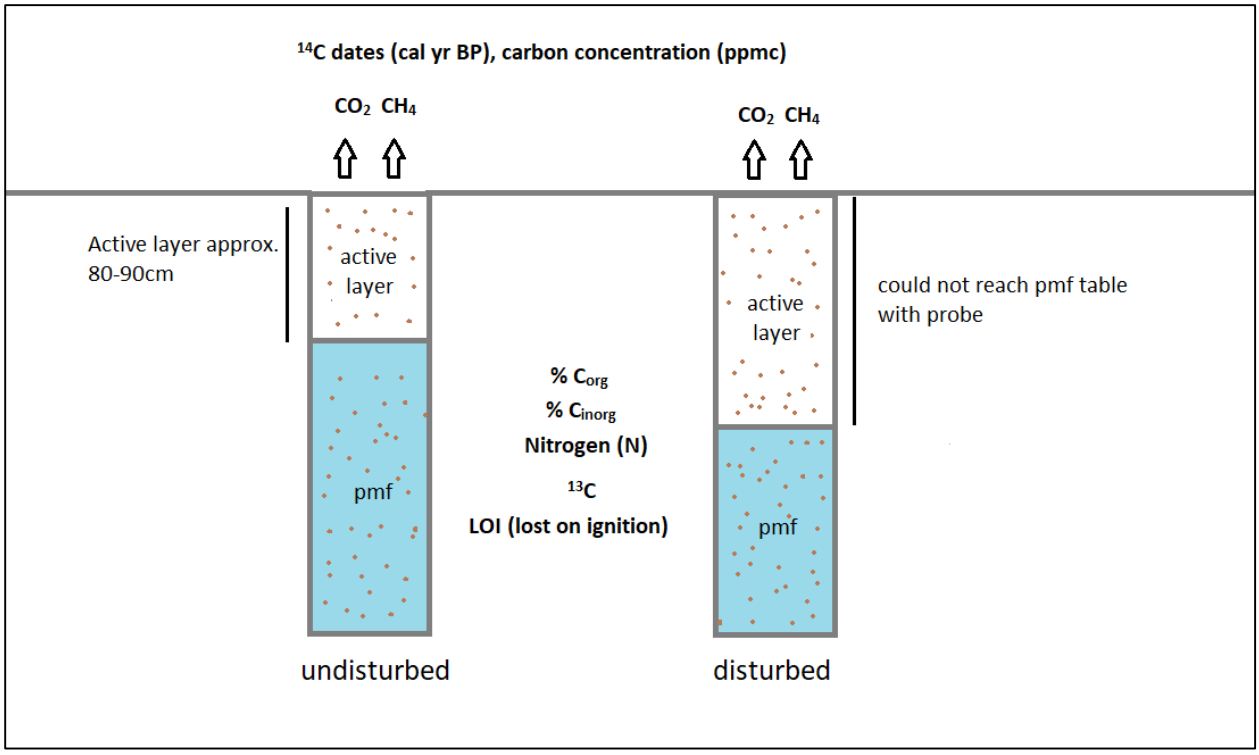

Figure 14. Conceptual model of undisturbed and disturbed sites.

4.2. Soil Gas Analysis

Soil gas emissions the ground surface were collected at 10 different sites with a gas flux chamber illustrated in Figure 15. The gas chambers were left installed for 24 hours to accumulate enough surface soil gas. Soil gas was collected from the chamber through a septum using a syringe needle connected to pre-evacuated and sterilized bottles through an evacuated polyethylene line connected to the syringe. Soil gas was also collected using a stainless steel tube with a fine screen connected at the end that was pushed into the soil and a plastic syringe connected to the top of the gas probe with a flexible tube (Figure 16). Gas collected with the soil gas probe with the syringe was then transferred to a pre-evacuated and sterilized bottle.

The soil gas samples were transported in cool conditions to the laboratories at the University of Ottawa. Soil gas sub-samples were passed through a GCI chromatograph to determine carbon concentrations ahead of a graphitization process. Samples with sufficient concentrations are sent to graphitization in preparation for ^{14}C carbon dating.

Figure 15. Gas flux chamber used to collect surface soil gas.

Figure 16. Shallow soil gas sampling with conventional soil gas probe.

The gas samples are currently in the process of analysis but several initial ^{14}C carbon dates are presented in Table 1. These initial analyses suggest that there is significant presence of young carbon in the soil gas being emitted at ground surface.

Sample	14C date (cal yr. BP)	±	F14C
GFC-01-01 (surface gas)	**265**	**25**	**0.9677**
SGP-01-01 (shallow gas ≈ 40-50cm depth)	**455**	**20**	**0.9452**

Table 1. 14C ages of 2 samples that yielded enough carbon concentration.

4.3 Surface Water and Groundwater Analysis

A total of 7 surface water samples and 4 groundwater samples were collected near to the coring and soil gas sampling locations along the all season road, roughly indicated on Figure 11. Shallow groundwater was collected using a drive-point stainless steel tube attached to a syringe for vacuum extraction. All water samples were collected and kept cool for shipping to the University of Ottawa's analytical laboratories. The samples are intended to provide basic shallow water geochemistry and isotopic composition to assist in determining the water source and in the interpretation of carbon flux to the ground surface, which will be part of the next stage of the research activities.

Figure 17 presents the stable isotope compositions of the surface water and groundwater. The data indicate a significant evaporation trend resulting in the concentration of the environmental water isotopes in both the surface waters and the groundwater. The initial geochemical analyses of the surface water samples indicate a high degree of variability in the chemical composition of the water which may reflect the nature of the local overburden mineralogy (Figure 18). Further analysis of the water samples is underway at the University of Ottawa.

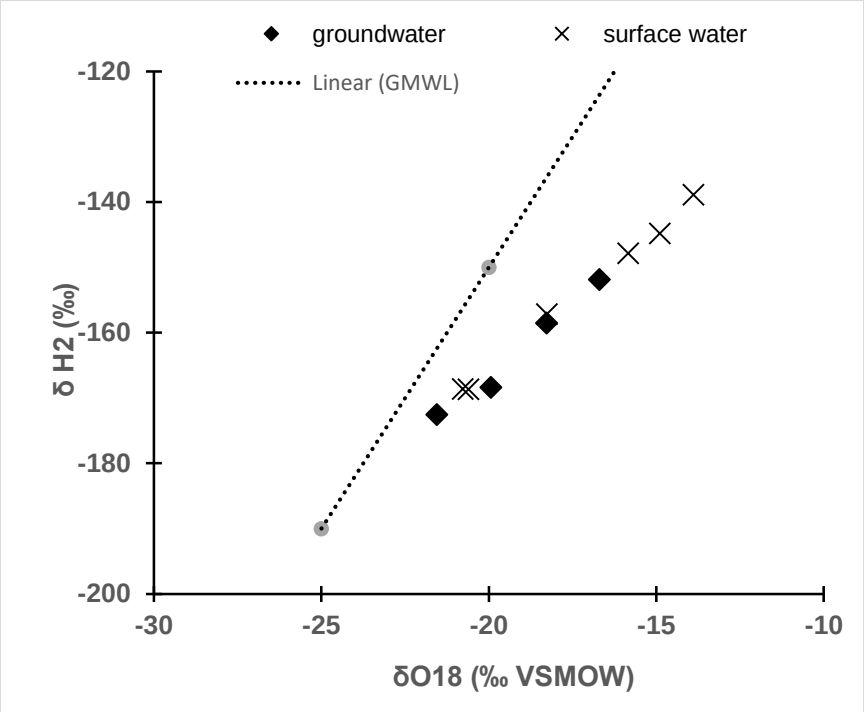

Figure 17. Graph showing δ H2 (‰) and δO18 (‰ VSMOW) of groundwater and surface water samples.

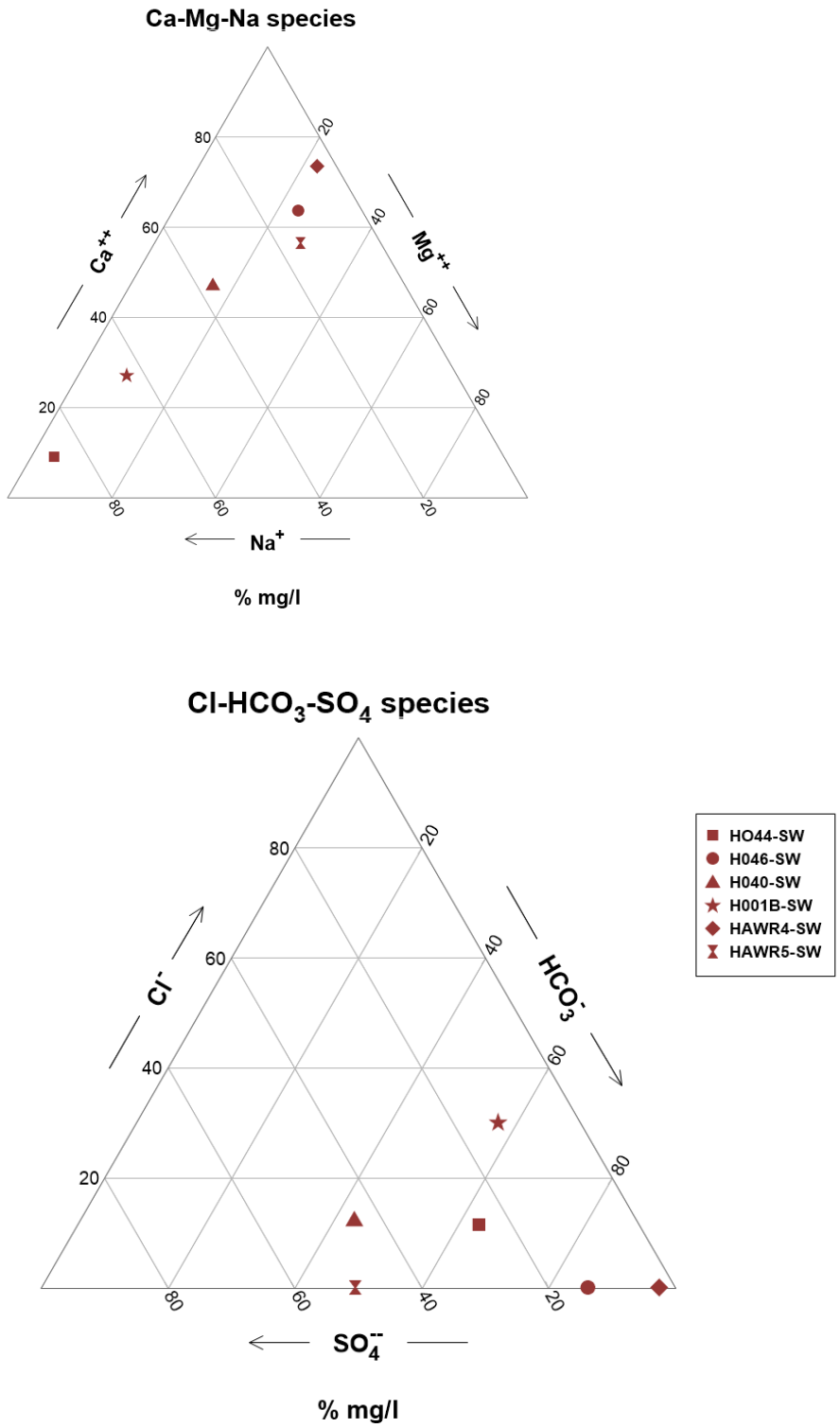

Figure 18. Ternary plots of basic analytes of surface water sampled in the 2023 field campaign.

5.0 Development and Initial Applications of Modeling Tools for Freeze-Thaw Processes

The modeling work over the Year 7 period involved both further developmental work and scenario testing with the simulators. The modeling tools, developed on the COMSOL Multiphysics platform and constructed as fully coupled thermal-hydraulic-mechanical-contaminant (THMC) formulation designed to simulate processes related to soil freeze-thaw dynamics and permafrost degradation have been advanced. The model is now capable of accommodating some aspects of reactive transport processes that are anticipated to be of interest in simulating carbon fate and transport. The main objective of the modeling work remains to analyze the role of transient, seasonal groundwater flow with respect to the short- and long-term fate of the discontinuous permafrost underlying the Bogg Creek watershed area. The simulation domain and numerical discretization used for the model experiments is shown in Figure 19.

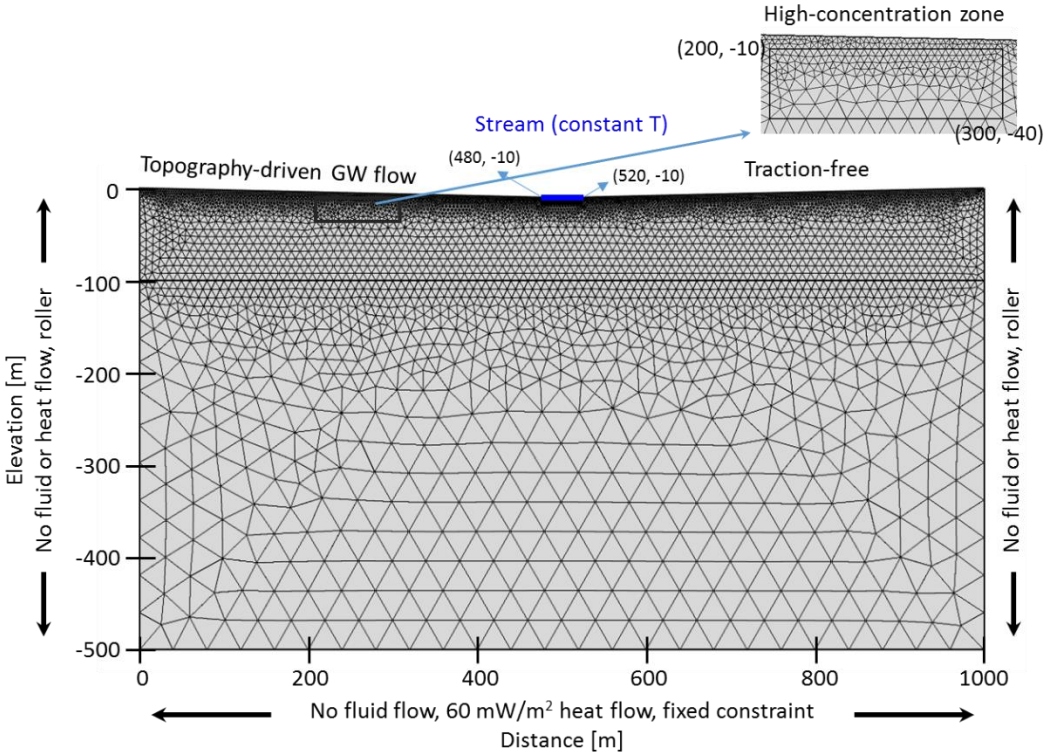

Figure 19. The geometry, mesh discretization and boundary conditions of the simulation domain. The blue line indicates the stream. The rectangle region denoted near the surface indicates the source region for the contaminant transport scenarios. Roller (vertical displacement only) and traction free (full displacement permitted) indicate boundary condition designations for the soil mechanics simulations (Huang and Rudolph, 2023).

With the model having been tested and verified with field and laboratory data (Huang and Rudolph, 2023)., the PhD student Ms. Jiaqi Weng has begun working on several scenarios of interest related to conditions representative of the Bogg Creek setting. The full suite of scenarios currently under consideration are contained Table 2. The main focus is on the influence of surface and subsurface heterogeneity, changes in temperature and hydraulic boundary conditions and the impact of warming climatic conditions. Initial results from several of the scenario simulations are presented below. A second major initiative within the modeling work of Ms. Weng, is the development of a simulation domain that

represents field conditions within Bogg Creek watershed. The focus is being placed along the all season road where the majority of the subsurface information is available on site. An example of the conceptual model that will be considered for this aspect of the modeling activity is shown in Figure 20 and this work is now underway.

Category			Scenarios
Soil and terrain configuration	Soil properties	Soil type	Consider different soil types commonly found in permafrost terrains
		Heterogeneity	Consider homogeneous or layered/heterogeneous soil configurations
	Topography	Surface shape	Include or exclude micro relief
		Surface slope	Consider gentle or steep topography
		Surface water body size	Include or exclude stream and lake geometry.
	Taliks		Include or exclude taliks
Land surface and subsurface temperature and hydraulic boundary conditions	Snow depth and vegetation		Compare surface condition assemblies found in the study site considering vegetation, land use, and human activities
	Regional flow		Include or exclude regional flow contribution to local groundwater system
Climate impact and soil freezing-thawing history	Climate	Summer length	Consider short (4 months) and long (8 month) summer condition
		Global warming	Consider different representative concentration pathways (RCPs)
		Deluge or drought	Consider common or deluge or drought year
	Soil history		Consider different SFCC

Table 2. Permafrost thaw scenarios under consideration for the numerical experimentation.

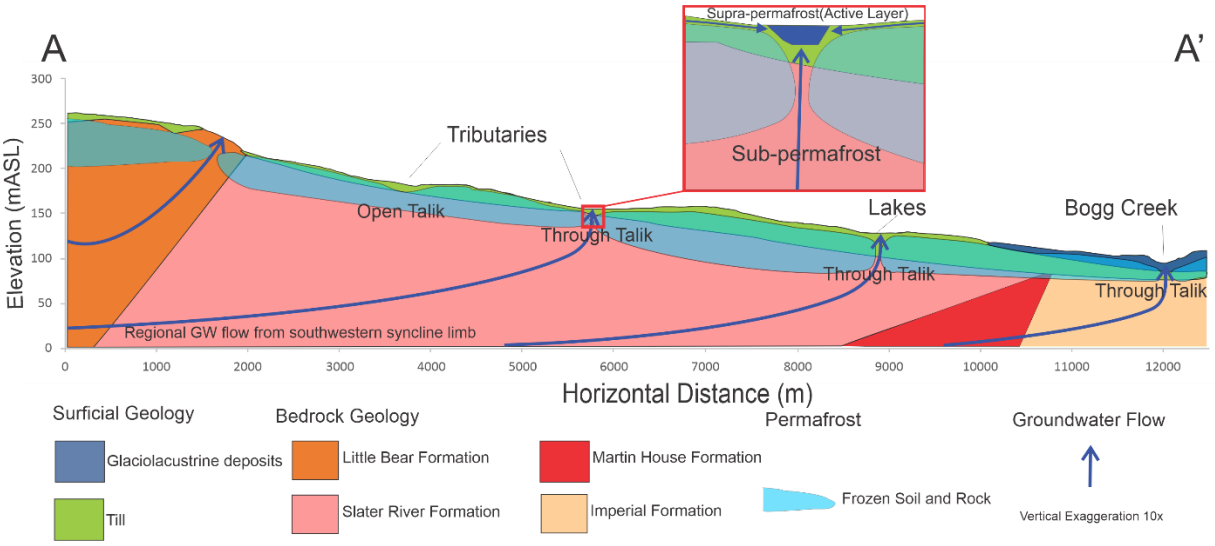

Figure 20. Conceptual model of the geologic setting, permafrost occurrence and regional groundwater flow system along the all season road within Bogg Creek watershed. This conceptual model will be the focus of numerical simulations investigating actual field conditions at the study site.

5.1. Influence of Regional Flow Magnitude and Soil Consolidation on Permafrost Degradation Rate

Initial scenario testing has involved examining the influence of the magnitude of the regional groundwater flow system and the compressibility of the soil, including deformation, on the rate of permafrost degradation. An initial condition developed after a period of 200 years of freezing at an annual air temperature of -2°C is shown in Figure 21 and represents the initial permafrost distribution. The annual air temperature is then raised to 1°C and the simulation is run until the permafrost has completely thawed.

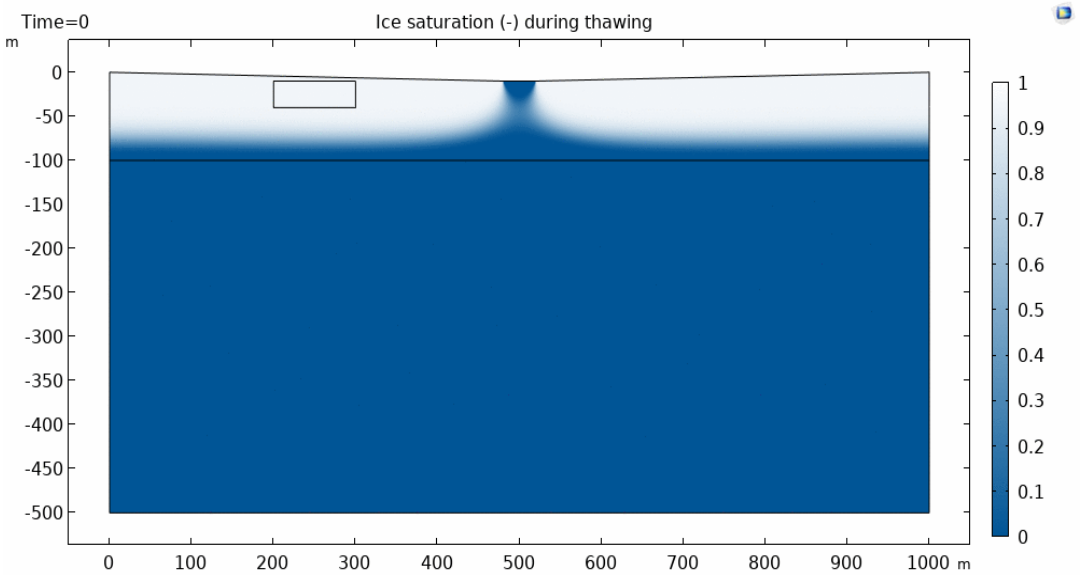

Figure 21. Initial steady ice saturation prior to the initiation of the thawing period.

In the first test scenario, the regional groundwater flow gradient was increased by a factor of two and as illustrated in Figure 22a, the ice saturation and permafrost disappearance rate increased significantly

illustrating the importance of groundwater flow velocity in degradation of permafrost. In the second example scenario, thaw rates in sand and clay soils were compared with sediment specific geotechnical parameters which control consolidation rate. The results presents in Figure 22b clearly illustrate a much more rapid degradation of permafrost in the sand soils, which indicates the significant role soil characteristics will have on permafrost thaw behavior. Other scenario experiments are currently underway.

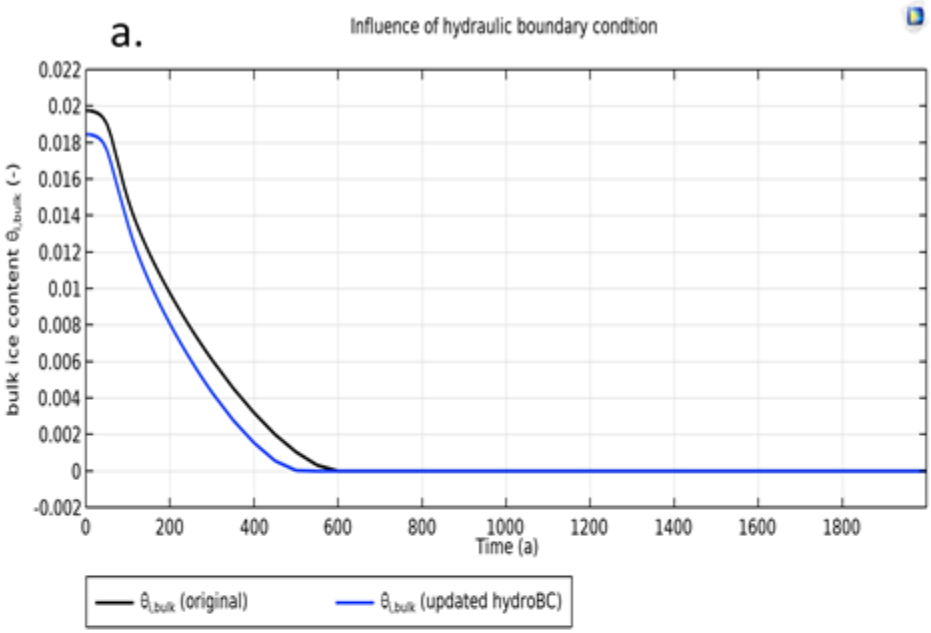

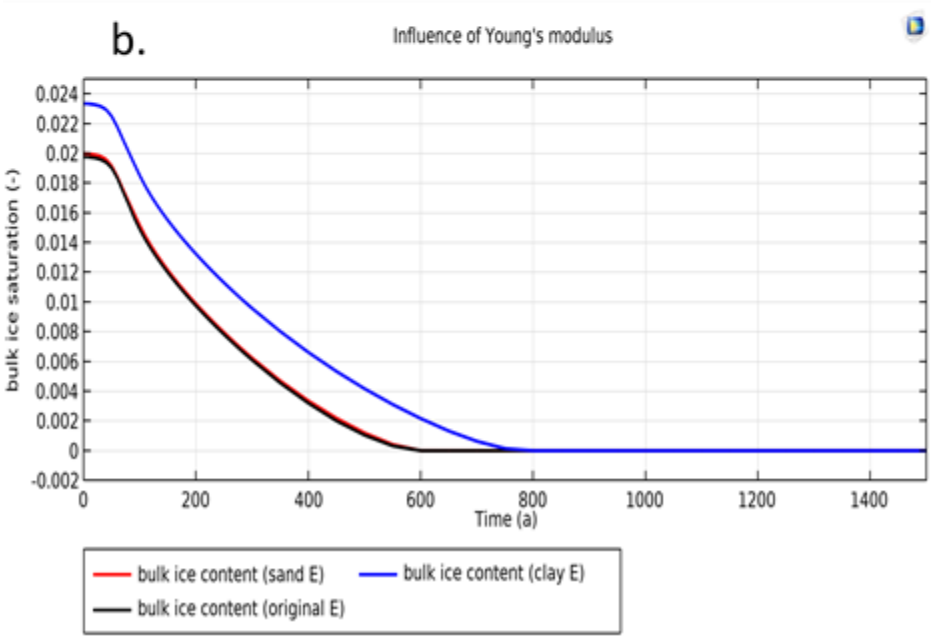

Figure 22. a. Permafrost degradation rate as a function of bulk ice content over time as influence by increased regional groundwater flow gradient or flow velocity. The higher groundwater flow rate results in more rapid thaw rate of the permafrost. b. Permafrost degradation rate as a function of bulk ice content

over time depending on soil type variability expressed by Young's modulus. Permafrost degradation rate was the slowest in the more compressible and less permeable clay sediments.

6.0 Proposed Year 8 Activities

Building on the results from the initial stage of this research project, the proposed work plan for Year 8 will focus on three main areas of study. The first component will involve enhanced and targeted applications of the series of advanced terrestrial geophysical instruments tested during the 2023 field season. These will be deployed at specific locations of interest (identified during the first phase of work), to better characterize the nature of the overburden materials with a specific focus on the occurrence of permafrost and the influence of land surface features and subsurface materials on permafrost continuity. Building on the experience from the 2023 summer season, the second component of the proposed field work will involve the mapping and characterizing of groundwater tracing tools to determine groundwater age, source and flow characteristics in a more precise fashion utilizing carbon isotopes, carbon species characterization and water chemistry. The gas sampling techniques have been enhanced and will be deployed at several new areas during the summer 2024 field program. Overall, the objectives of these field activities will be to: 1). more specifically quantify the geologic conditions and the nature of carbon within the subsurface and being released to the atmosphere; 2). continue to improve the understanding of the groundwater and surface water interactions and 3). Develop further insight into the nature and distribution of permafrost at the watershed scale. This improved understanding will be used to inform the numerical modeling tools designed to simulate critical future scenarios of interest to the entire collaborative team, within the context of a warming climate. The continued scenario modeling work represents the third major component of the proposed work plan for Year 7.

7.0 Community Participation

One of the main communication mechanisms with our community groups has been through video conferences and written document sharing. As part of the Research Licensing process, an update on our research progress and results have been shared with our colleagues from the Sahtu Renewable Resources Board, Tulita Renewable Resources Council and the Norman Wells Renewable Resources Council. In preparation for the Summer 2024 field season, project results contained in this annual report will be shared with these two groups and the proposed 2024 work program will be presented and discussed during a virtual meeting planned for mid-May, 2024. As with our previous meetings, we will request suggestions and guidance from the community leaders on priority topics to focus on as part of the continued research program. We are also planning to provide an in-person presentation of the results and current activities while visiting Norman Wells, which will include a demonstration of the field equipment for both the Board members and local youth who may have an interest.

6.0 References

Herring, T., Lewkowicz, A.G., Hauck, C., Hilbich, C., Mollaret, C., Oldenborger, G.A., Uhlemann, S., Farzamian, M., Calmels, F., and Scandroglio, R. (2023). Best practices for using electrical resistivity tomography to investigate permafrost. Permafrost and Periglacial Processes. 34:4. 494-512. https://doi.org/10.1002/ppp.2207.

Holloway J.E. and Lewkowicz A.G. (2020). Half a century of discontinuous permafrost persistence and degradation in western Canada. Permafrost and periglacial processes. 31(1):85-96. doi:10.1002/ppp.2017.

Project Publications

Huang, X. and Rudolph, D. L., 2023. Numerical study of coupled water and vapour flow, heat transfer, and solute transport in variably-saturated deformable soil during freeze-thaw cycles, Water Resources Research, 59, e2022WR032146. https://doi.org/10.1029/2022WR032146.

Rudolph, D. L., 2023. Groundwater, The Invisible Component of the Water Cycle, 14th Annual NWT Water Stewardship Strategy Implementation Workshop Inspiring our Future Water Stewards, Yellowknife, Oct.

Rudolph, D. L., 2024. Awakening a Giant! Impacts of permafrost degradation on groundwater in the North, Northern Water Resources and Climate Change, Laurier Northern Webinar Series, March, (Invited).

Wiebe, A.J.1,2, McKenzie, J.M. 2, Hamel, E. 2, Yin, H. 1, Rudolph, D.L. 1, Stribling, S. 2, Mulligan, B. 3, and de Grandpré, I.4, 2023. Advancing groundwater vulnerability assessment in the Yukon and Northwest Territories, Global Water Futures Annual Science Meeting, Saskatoon, Sask.